Study on Fracture Propagation and Productivity Prediction of Network Fracturing in Tight Oil Reservoir

Lin Wu[1,a,*], Liqiang Zhao[1,b]

[1]State Key Laboratory of Oil and Gas Reservoir Geology and Exploitation, Southwest Petroleum University, Chengdu 610500, China.

[a]sgywlin@163.com, [b]zhaolq@vip.163.com

Abstract

In this paper, an integrated model for fracture propagation and productivity prediction of network fracturing in tight reservoir was established, and the stress field was solved by displacement discontinuity method, and the flow field was solved by finite difference method. The reliability of the model was verified, and the influence of construction parameters and formation parameters on fracture network morphology and productivity of network fracturing was studied. Parameter sensitivity analysis results show that under the same conditions of other parameters, the larger the displacement, the larger the fracturing fluid volume, the smaller the viscosity of the fracturing fluid and the smaller the in-situ stress difference, the larger the total fracture length and the greater the productivity of the stimulated well, but the average fracture opening is not necessarily larger, and its value is affected by the angle between the natural fracture and the maximum horizontal principal stress and the connection between the hydraulic fracture and the natural fracture. This study can provide some theoretical guidance for network fracturing optimization design and efficient development of tight oil reservoir.

Keywords

Network fracturing; Fracture propagation; Fracture network morphology; Productivity prediction; Displacement discontinuity method; Embedded discrete fracture model.

1. Introduction

Tight reservoir has the characteristics of low porosity and low permeability, which can't realize its commercial value by using the conventional stimulation method of symmetrical double wing fracture, so it usually needs fracture network fracturing to obtain industrial production capacity [1-2]. At present, there have been a lot of numerical simulation studies on fracture propagation and productivity prediction of fracture network fracturing, but scholars basically divide fracture propagation and productivity prediction of fracture network fracturing into two independent parts for research, that is, in the process of fracture propagation simulation of fracture network fracturing, the SRV is taken as the optimized target parameter [3-5]; in the process of productivity prediction, the fracture network shape is assumed for simulation, instead of directly obtaining the fracture morphology at the end of fracture propagation [6-8]. The fracture morphology directly affects the productivity, so the fracture propagation and productivity prediction should be unified for research, but at present, the research on the integration of fracture propagation and productivity prediction is relatively less [9-12].

Therefore, this study established a set of integrated model for fracture propagation and productivity prediction of fracture network fracturing in tight reservoir, analyzed the influence rule of construction parameters and formation parameters on fracture network morphology

2. Mathematical Model

2.1 Mechanical model of fracture propagation

This section will introduce the fracture propagation mechanics solution method, the fracture propagation diverting criterion and the fracture intersection criterion.

2.1.1 Displacement discontinuity method

In this study, the displacement discontinuity method is used to solve the fracture propagation mechanics.

In displacement discontinuity method, the influence of finite fracture height on stress field and displacement field is considered. After boundary conditions are added, the induced stress can be expressed as [13]:

$$\begin{cases} \sum_{j=1}^{N}\left(G^{ij}A_{ss}^{ij}D_s^j+G^{ij}A_{sn}^{ij}D_n^j\right)=-\frac{1}{2}\left(\sigma_H-\sigma_h\right)\sin 2\theta_i-\sigma_{xy}\cos 2\theta_i \\ \sum_{j=1}^{N}\left(G^{ij}A_{ns}^{ij}D_s^j+G^{ij}A_{nn}^{ij}D_n^j\right)=P_{frc}^i-\sigma_H\sin^2\theta_i-\sigma_h\cos^2\theta_i+\sigma_{xy}\sin 2\theta_i \end{cases} \quad (i,j=1,2,\cdots,N) \tag{1}$$

Where, σ_s^i、σ_n^i are the tangential and normal induced stress of element *i*, Pa; A_{ss}^{ij}、A_{ns}^{ij}、A_{sn}^{ij}、A_{nn}^{ij} are the influence coefficient of boundary stress, Pa.m^{-1}; D_s^j、D_n^j are the tangent displacement discontinuity and normal displacement discontinuity of element *j*, m; G is the three-dimensional correction coefficient, dimensionless; σ_H is the maximum principal stress in the far field, Pa; σ_h is the minimum principal stress in the far field, Pa; σ_{xy} is the far-field shear stress, Pa; P_{frc}^i is the fluid pressure in fracture unit *i*, Pa; θ_i is the angle between crack element *i* and x-axis.

In formula (1), there are 2*N* unknowns and 2*N* equations in total. The displacement discontinuities *Ds* and *Dn* of each fracture element can be calculated by solving the equations.

2.1.2 Fracture propagation and diverting criterion

The stress intensity factor is calculated according to the displacement discontinuity of the tip element [14]:

$$\begin{aligned} K_{\mathrm{I}} &= \frac{0.806E\sqrt{\pi}}{4\left(1-\nu^2\right)\sqrt{2a}}D_n^t \\ K_{\mathrm{II}} &= \frac{0.806E\sqrt{\pi}}{4\left(1-\nu^2\right)\sqrt{2a}}D_s^t \end{aligned} \tag{2}$$

Where, K_I is the first type of stress intensity factor, Pa.m$^{1/2}$; K_{II} is the second type of stress intensity factor, Pa.m$^{1/2}$; *E* is the modulus of elasticity, Pa; *v* is Poisson's ratio, dimensionless; *a* is the half length of fracture tip element, m; D_n^t is the normal displacement of fracture tip element, m; D_s^t is the tangential displacement of fracture tip element, m.

According to the maximum circumferential stress criterion, the fracture propagates along the direction of the maximum circumferential stress, which can be determined by the stress intensity factor [15]:

$$\theta=\begin{cases} 0 & \left(K_{\mathrm{II}}=0\right) \\ 2\arctan\left(\frac{1}{4}\left(\frac{K_{\mathrm{I}}}{K_{\mathrm{II}}}-\mathrm{sgn}\left(K_{\mathrm{II}}\right)\sqrt{\left(\frac{K_{\mathrm{I}}}{K_{\mathrm{II}}}\right)^2+8}\right)\right) & \left(K_{\mathrm{II}}\neq 0\right) \end{cases} \tag{3}$$

Where, θ is the deflection angle of fracture propagation direction in polar coordinate system of tip, rad.

2.1.3 Fracture interaction criteria

Based on the Gu model, Zeng Qingdong et al. established the interaction criterion [16] considering the change of fluid pressure on the natural fracture interface, which is more in line with the actual situation of fracture intersection. Therefore, this criterion is used for judgment in this paper.

According to the Coulomb Navier criterion, the friction interface does not slip, which needs to meet the following requirements:

$$\left|\tau_\beta\right|<S_0+\mu_f\sigma_{\beta y} \tag{4}$$

Where, τ_β is the shear stress on the natural fracture surface, Pa; S_0 is the cohesion of the natural fracture, Pa; μ_f is the friction coefficient of the natural fracture, dimensionless; $\sigma_{\beta y}$ is the normal stress on the natural fracture surface, Pa.

If equation (4) is satisfied, it means that there is no sliding between the natural fracture surfaces, and the tensile principal stress on the other side of the natural fracture overcomes the tensile strength of the rock, that is to say, the hydraulic fracture passes through the natural fracture, and continues to propagate on the other side of the natural fracture. If formula (4) is not satisfied, it means that the hydraulic fracture does not start to propagate again on the other side of the natural fracture, that is, it does not pass through the natural fracture, but diverts to propagate along the natural fracture.

2.2 Fluid flow model

2.2.1 Fluid flow model during fracturing

It is assumed that the fracture fluid is incompressible Newton fluid, there is no gap between the fluid tip and the fracture tip, and the fracture fluid fills the whole fracture. Then the flow equation in the fracture can be expressed as [17]:

$$\frac{\partial w}{\partial t}+q_l=\frac{1}{12\mu}\left(w^3\frac{\partial p}{\partial s}\right) \tag{5}$$

Where, q is the fluid flow rate in the fracture, m^2/s; p is the fluid fracturing in the fracture, Pa; μ is the viscosity of the fracturing fluid, mPa.s; w is the fracture width, m; s is the length in the fracture propagation direction, m; t is the time, s; q_l is the filtration coefficient (obtained from the embedded discrete fracture model), m/s.

In addition, the fracturing fluid shall meet the overall mass conservation equation:

$$\int_0^l Hw(s,t)ds+\int_0^l\int_0^t q_l dtds=\int_0^t q_0 dt \tag{6}$$

Where, H is the fracture height, m; l is the fracture length, m; q_0 is the injection flow at the wellbore, m^3/s.

The initial conditions and boundary conditions are as follows: the initial fracture width is assumed to be 0, the fracture tip width is 0, the fracture tip flow rate is 0, and the flow rate at wellbore is *q0*.

$$\begin{cases} w(s,0)=0 \\ w(l,t)=0 \\ q(0,t)=q_0 \\ q(l,t)=0 \end{cases} \tag{7}$$

In the fracturing process, the gravity of the fracturing fluid lost to the matrix is ignored, and if the single-phase flow is assumed, the two-dimensional seepage differential equation in the matrix is:

$$\nabla\cdot\left[\frac{K_m\rho_{ff}}{\mu_{ff}}\nabla p_m\right]+q_l=\frac{\partial}{\partial t}\left(\phi_m\rho_{ff}\right) \tag{8}$$

Where, K_m is matrix permeability, m^2; ρ_{ff} is density of fracturing fluid, kg/m^3; u_{ff} is viscosity of fracturing fluid, Pa.s; p_m is fluid pressure in matrix, Pa; φ_m is matrix porosity.

The initial condition is:

$$p_m|_{t=0}=p_{m0} \tag{9}$$

Where, p_{m0} is the initial fluid pressure in the matrix, Pa.

The external boundary condition is:

$$p_m|_{out}=p_{m0} \tag{10}$$

2.2.2 Fluid flow model during production

Because the migration and settlement of proppant are not considered in the numerical model of fracture propagation, the conductivity of proppant fracture cannot be simulated strictly. Therefore, this study assumes that the fracture morphology formed after the construction is the final supporting fracture morphology, and the fracture width and permeability in the fracture conform to the cubic law, then the permeability in the fracture can be expressed as [18]:

$$K_f = f \cdot \frac{w^2}{12} \tag{11}$$

Where, f is the correction factor, dimensionless.

If the non Darcy flow and the gravity of the fluid in the fracture are ignored, and the single-phase flow is assumed, the differential equation of seepage in the fracture during the production process is as follows:

$$\nabla \cdot \left[\frac{K_f \rho_o}{\mu_o} \nabla p_f \right] + q_o + Q_o = \frac{\partial}{\partial t}\left(\phi_f \rho_o \right) \tag{12}$$

Where, K_f is fracture permeability, m^2; ρ_o is density o f crude oil, kg/m^3; μ_o is viscosity of crude oil, Pa.s; p_f is fluid pressure in fracture, Pa; q_o is matrix fracture flow, $kg/(m^3\ s)$; Qo is crude oil production, $kg/(m^3\ s)$; φ_f is fracture porosity, dimensionless.

When the gravity of the fluid is ignored and single-phase flow is assumed, the seepage differential equation in the matrix during the production process is as follows:

$$\nabla \cdot \left[\frac{K_m \rho_o}{\mu_o} \nabla p_m \right] - q_o + Q_o = \frac{\partial}{\partial t}\left(\phi_m \rho_o \right) \tag{13}$$

The initial condition in the production process is:

$$p_m \mid_{t=0} = p_{fe0} \tag{14}$$

Where, p_{fe0} is the fluid pressure in the matrix after fracturing, Pa.

The internal and external boundary conditions in the production process are:

$$\begin{aligned} p_f \mid_{in} &= p_{wf} \\ p_m \mid_{out} &= p_{m0} \end{aligned} \tag{15}$$

Where, p_{wf} is bottom hole flow pressure, pa.

The fluid flow models are solved by finite difference method.

2.3 Embedded discrete fracture model

The embedded discrete fracture model (EDFM) defines the non-neighboring connections (NNC). The significance of the introduction of NNC is to allow flux exchange between adjacent grids in the physical model but not adjacent grids in the computational model [19]. The grids involved in each NNC pair are connected by conductivity coefficient. After introducing conductivity coefficient, the volume flow of a phase n between two grids connected by a NNC pair is:

$$q_n = \frac{K_{mrn}}{\mu_n} T_{NNC} \Delta P \tag{16}$$

Where, K_{mrn} is the relative permeability of phase n, dimensionless; μ_n is the viscosity of phase n, Pa.s; T_{NNC} is the conductivity of NNC pair, mD m; ΔP is the pressure difference between two grids, Pa.

In the embedded discrete fracture, after the matrix grid boundary divides the fracture, three kinds of non adjacent connection pairs will be formed, that is, between the fracture and matrix, between the

fracture segments intersecting the fracture, and between the fracture segments in a certain fracture. The general formula for calculating the conductivity coefficient of non adjacent connection pairs is [20]:

$$T_{NNC} = \frac{k_{NNC} A_{NNC}}{d_{NNC}} \tag{17}$$

Where, k_{NNC} is NNC pair permeability, mD; A_{NNC} is NNC pair contact area, m^2; d_{NNC} is the characteristic distance related to NNC connection pair, m.

3. Research Route

The integrated research route of fracture propagation and productivity prediction of fracture network fracturing in tight reservoir are as follows:

(1) According to the measured data of natural fractures in the reservoir, the network model of natural fractures in the reservoir is constructed;

(2) Combined with the natural fracture network model, the fracture network of tight reservoir is simulated and the complex fracture network is obtained;

(3) The fracture network (natural fracture and hydraulic fracture) is represented by the embedded discrete fracture model, and the fracture network data is applied to the productivity prediction model to calculate the oil well productivity under such fracture network;

(4) Parameter sensitivity analysis of construction parameters, formation parameters on the fracture network morphology and productivity.

4. Numerical Model Verification

This section will verify the fracture propagation model and productivity model respectively. Because the fracture propagation model in this paper assumes that the flow in the fracture is a plate flow, and the vertical section is rectangular, so KGD model is selected to verify. During the validation, the parameter values are shown in Table 1. At the same time, the single fracture vertical well is used for constant pressure production, and the calculation results in this paper are compared with those in Eclipse to verify the productivity model. The parameter values are shown in Table 2.

Table 1 Parameters required for fracture propagation model verification

Young's modulus（MPa）	2.8×10^4	Poisson's ratio	0.21
Construction displacement（m^3/min）	5	Fluid viscosity（mPa.s）	60
Height（m）	50	Filtration coefficient（$m/min^{0.5}$）	3×10^{-4}

Table 2 Parameters required for productivity model validation

Reservoir size（m^2）	1000×1000	Reservoir thickness（m）	20
Crude oil density（kg/m^3）	850	Volume coefficient of crude oil	1.2
Compressibility of crude oil（MPa^{-1}）	1.5×10^{-3}	Viscosity of crude oil（mPa.s）	14
Matrix permeability（mD）	0.8	Matrix porosity	0.13
Original reservoir pressure（MPa）	24	Bottom hole flow pressure（MPa）	18
Half length of hydraulic fracture（m）	70	Width of hydraulic fracture（m）	0.008
Hydraulic fracture permeability（mD）	3.5×10^4	Well radius（m）	0.12

Compared with KGD model, the difference between the two models in the initial stage is smaller, and the error increases gradually with the increase of fracture length. Because KGD model assumes

that the fracture plane strain is on the horizontal plane, and the fracture opening along the direction of fracture height is constant, the calculation result of KGD model should be more accurate when the hydraulic fracture length is less than or equal to the height. The difference between this model and KGD model is small, so the model has high reliability.

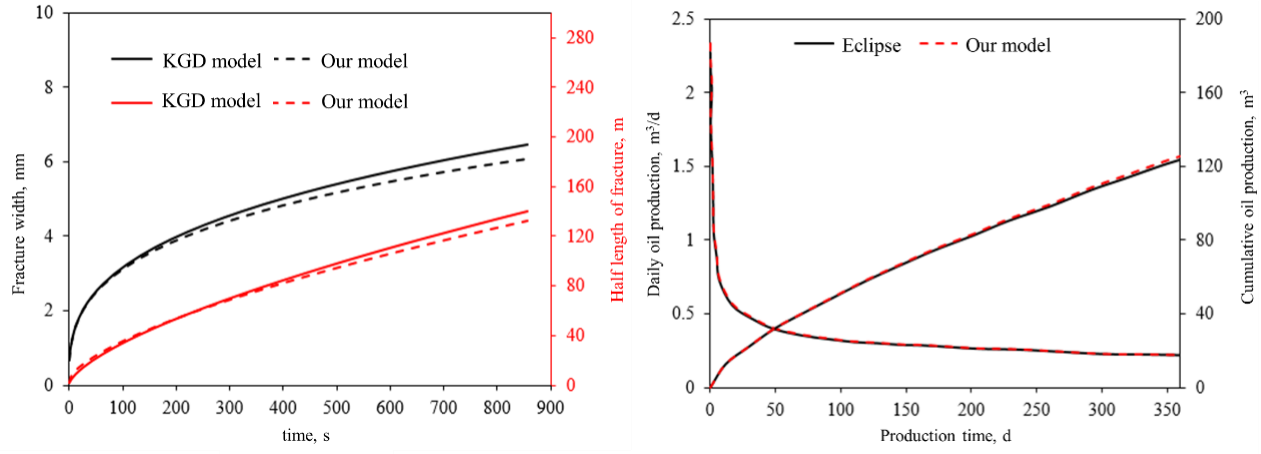

Figure 1 Model validation results

The daily oil production and cumulative oil production calculated by the productivity model in this paper are basically the same as those calculated by Eclipse, so the correctness of the productivity model in this paper can be explained.

5. Example Analysis

In this section, through the integrated model of fracture propagation and productivity prediction in tight reservoir, the propagation behavior of complex fractures in fracture network fracturing in tight reservoir will be simulated, and the influence of construction parameters and formation parameters on fracture network morphology and productivity will be analyzed.

5.1 Natural fracture network

The parameters of a well area in L oilfield are used for simulation, and the natural fracture parameters in the studied area are shown in Table 3.

We use the data in Table 3 to build the natural fracture network model of the reservoir, as shown in Figure 2, and the well hole is located (400m, 400m).

Table 3 Natural fracture parameters in the area

Parameter	Value		Parameter	Value	
Area length (m)	800		Area width (m)	800	
Fracture opening (μm)	Law of distribution	Normal distribution	Fracture length(m)	Law of distribution	Normal distribution
	Mean value	43		Mean value	23.05
	Standard deviation	23		Standard deviation	10.12
Fracture angle (°)	Law of distribution	Fisher distribution	Fracture location	Law of distribution	Uniform distribution
	Mean value	45	Fracture density (/m)	1.0	
	K	12			

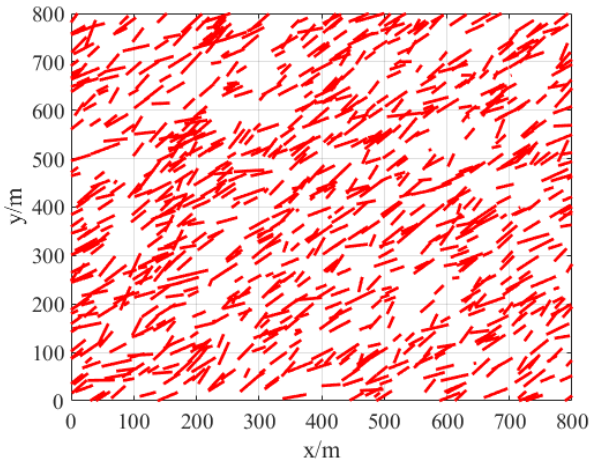

Figure 2 Distribution of natural fractures in the area

5.2 Parameter sensitivity analysis

In this section, single factor analysis is mainly used to analyze the influence of construction displacement, volume of fracturing fluid, viscosity of fracturing fluid and in-stu stress difference on fracture morphology and productivity. See Table 4 for target reservoir parameters.

Table 4 Basic data of the reservoir

Original formation pressure (MPa)	65.1	Bottom hole flow pressure (MPa)	52.1
Matrix permeability (mD)	2.1	Matrix porosity (%)	8.3
Reservoir thickness (m)	20	Well radius (m)	0.1
Crude oil density (kg/m^3)	850	Volume coefficient of crude oil	1.2
Compressibility of crude oil (MPa^{-1})	1.2×10^{-3}	Viscosity of crude oil (mPa.s)	14
Maximum principal stress (MPa)	104	Minimum principal stress (MPa)	94
Young's modulus (MPa)	2.8×10^4	Poisson's ratio	0.21
Tensile strength of rock (MPa)	3	Cohesion (MPa)	3
Friction coefficient	0.6	Viscosity of fracturing fluid (mPa.s)	10
Construction displacement (m^3/min)	10	Volume of fracturing fluid (m^3)	800

5.2.1 Construction displacement

In the process of analyzing the influence of construction displacement on fracture morphology and productivity, the remaining parameters remain unchanged, and the simulation results are shown in Figure 3.

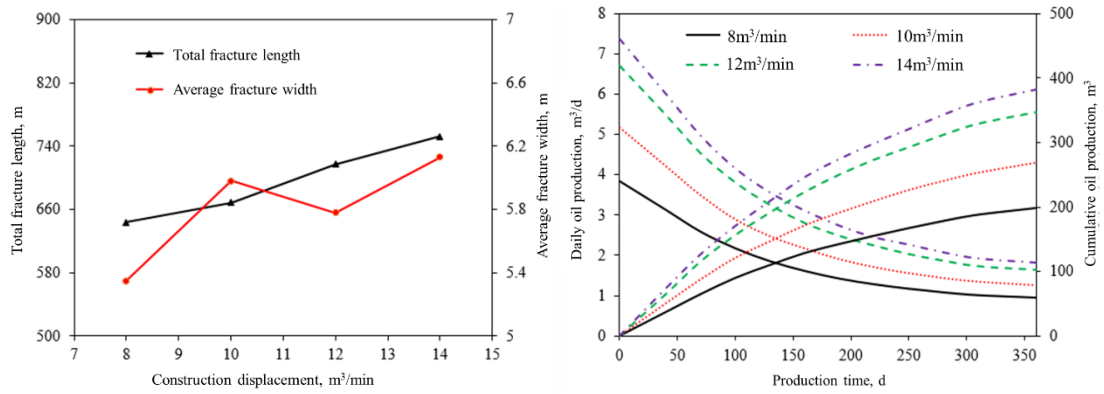

Figure 3 Influence of displacement on fracture parameters and productivity

With the increase of displacement, the total length of fractures increases, but the average fracture opening does not always increase. Although the increase of displacement will increase the propagation length of each branch fracture, part of the branch fractures will be caught by the natural fractures and propagate along the natural fractures. The normal stress of the hydraulic fractures propagating along the natural fractures is large, and the fracture opening is relatively small, so the average fracture opening is reduced, as shown in the figure. However, with a large displacement, the opening of the main fracture and each main branch fracture has increased significantly, that is, the main seepage channel has a better conductivity. Therefore, under the same total injection amount, increasing the displacement will increase the total fracture length and the opening of the main fracture section in the fracture network, and the productivity of the stimulated well will be improved.

5.2.2 Volume of fracturing fluid

In the process of analyzing the effect of volume of fracturing fluid on fracture morphology and productivity, the remaining parameters remain unchanged, and the simulation results are shown in Figure 4.

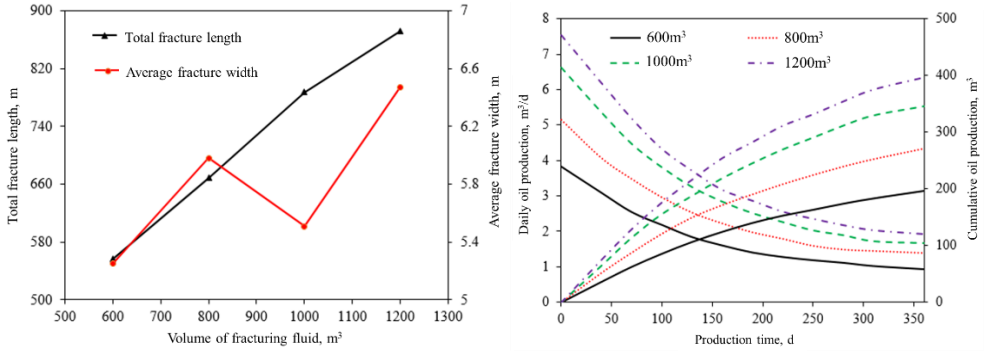

Figure 4 Influence of fracturing fluid volume on fracture parameters and productivity

The volume of fracturing fluid has a great influence on the fracture network morphology. The increase of the volume of fracturing fluid will increase the total fracture length in the fracture network, but the average fracture opening does not always increase. However, with the same other parameters, increasing the liquid volume will increase the total fracture length and the opening of the main fracture section in the fracture network, and improve the productivity of the stimulated well.

5.2.3 Viscosity of fracturing fluid

In the process of analyzing the influence of fracturing fluid viscosity on fracture morphology and productivity, the remaining parameters remain unchanged, and the simulation results are shown in Figure 5.

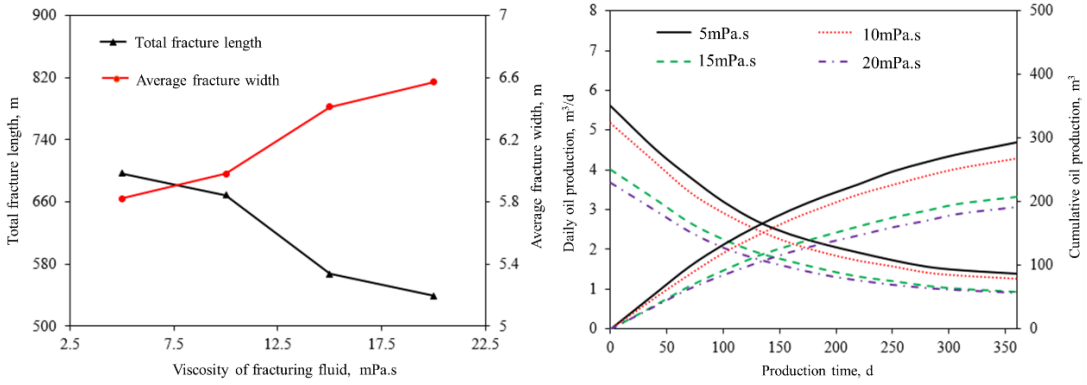

Figure 5 Influence of fracturing fluid viscosity on fracture parameters and productivity

With the increase of the viscosity of the fracturing fluid, the total fracture length decreases gradually, and the average fracture opening increase gradually. This is because when the viscosity of the

fracturing fluid increases, the flow performance of the fracturing fluid in the fracture becomes poor, the pressure drop increases, and the fracture extension ability decreases, which limits the fracture propagation in the length direction, and the increased pressure drop makes the fracture effectively propagate in the width. On the other hand, when the viscosity of the fracturing fluid increases to a certain value, the natural fracture communicating decreases, and the proportion of the natural fracture communicating to the total fracture length decreases, so the average fracture opening increases.

When the fracture length decreases, the productivity will decrease, and the productivity will increase with the increase of fracture opening. However, from Figure 5, it can be seen that the influence of length is greater than that of opening. Therefore, in the low-permeability tight reservoir, the fracturing fluid with low viscosity should be used in the fracture network fracturing process to open more natural fractures and increase the total length of fractures, so as to improve the productivity of the stimulated wells.

5.2.4 In-situ stress difference

In the process of analyzing the influence of in-situ stress difference on fracture morphology and productivity, the remaining parameters remain unchanged, and the simulation results are shown in Figure 6.

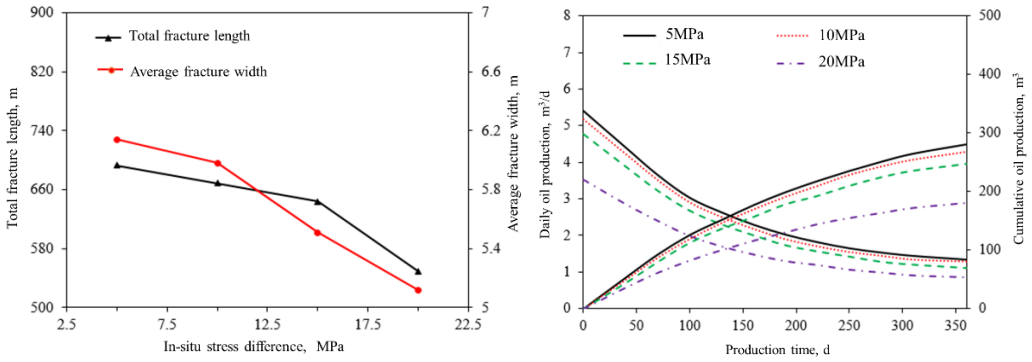

Figure 6 Influence of in-situ stress difference on fracture parameters and productivity

With the increase of in-situ stress difference, the total fracture length and average fracture opening decrease. When the local stress difference is large, the normal stress of natural fractures is large. Even under the action of high net pressure, some natural fractures are difficult to be opened, so the total fracture length will drop sharply. With the decrease of the length of the open natural fracture, the proportion of the main fracture increases, and the average fracture opening will increase, but with the decrease of the total fracture length, the main fracture opening will decrease, and the average fracture opening will decrease. It can be seen from the figure that the influence of the latter is greater than that of the former, so the average fracture opening will decrease.

With the increase of in-situ stress difference, even with the same reconstruction scale, the total fracture length and average fracture opening will be reduced, so the productivity of the transformed well will also be reduced. When the in-situ stress difference increases to a certain value, the productivity will drop sharply. Therefore, in the high stress difference reservoir, on the premise of considering economy and safety, the reconstruction scale should be increased as much as possible to maximize the use of the reservoir.

6. Conclusions

In this study, an integrated model of fracture propagation and productivity prediction of fracture network fracturing in tight reservoir is established. The influence of construction parameters and formation parameters on fracture network shape and productivity is analyzed by single factor. The research conclusion can provide certain theoretical reference for fracture network fracturing optimal design and efficient development in tight reservoir. The specific conclusions are as follows:

(1) In the case of the same other parameters, the larger the construction displacement, the larger the volume of fracturing fluid, the smaller the viscosity of fracturing fluid and the smaller the difference in-situ stress, the larger the total fracture length and the greater the productivity of fracture network fracturing, but the average fracture opening is not necessarily larger, and its value is affected by the angle between the natural fracture and the maximum horizontal principal stress and the communication between the artificial fracture and the natural fracture.

(2) If the construction equipment capacity, wellbore conditions and geomechanics conditions permit, properly increasing the fracturing construction displacement and fracturing fluid volume is conducive to improving the single well productivity. In the high stress difference reservoir, a larger scale of reconstruction is needed, but the scale of reconstruction should also match the parameters of the reservoir.

References

[1] Shi Xiaodong. Productivity Forecast of Vertical Well with Multi-Layer Network Fracturing in Tight Oil Reservoir [J]. Special Oil & Gas Reservoirs, 2017(1).

[2] Zhang Yong, Wang Zhisheng, Gan Yuming, et al. Feasibility study and application of fracture network fracturing technology for high stress difference fracture reservoir [J]. Drilling & Production Technology, 2019 (4)

[3] Zhang S C, Lei X, Zhou Y S, et al. Numerical simulation of hydraulic fracture propagation in tight oil reservoirs by volumetric fracturing[J]. Petroleum Science, 2015, 12(4):674-682.

[4] Peng Jiao. Study on the main factors affecting the volume of reservoir reconstruction by fracture network fracturing in tight reservoir [D]. Xi'an University of Petroleum, 2016

[5] He Shuangxi, Wang Tengfei, Yan Xiangyang, et al. Analysis of network fracturing numerical simulation in CBM reservoi [J]. Reservoir Evaluation and Development, 2017, 7 (3): 74-78

[6] Xu Linjing. Prediction of volume fracturing productivity in tight reservoirs [D]. China University of Petroleum (Beijing), 2016

[7] Ren Dengfeng. Fracture network fracturing productivity simulation of fractured tight gas reservoir [D]. Southwest Petroleum University, 2014

[8] Zhang Lihui, Liu Sha, Yong Rui, et al. EDFM-based Numerical Simulation of Horizontal Wells with Multi-stage Hydraulic Fracturing in Tight Reservoirs [J].

[9] Journal of Southwest Petroleum University(Science & Technology Edition), 2019 (4): 1-11

[10] Ren long. Fracture pattern expansion and fluid solid full coupling productivity prediction of volume fracturing horizontal wells in tight reservoirs [D]. China University of Petroleum (East China), 2016

[11] Zhou Xiang, Zhang Shicheng, Zou Yushi, et al. Volume fracturing fracture propagation and productivity simulation of horizontal wells in tight reservoirs [J].

[12] Journal of Xi'an Shiyou University(Natural Science), 2015, 30 (4): 53-58

[13] Zeng Q, Yao J. Numerical simulation of fracture network generation in naturally fractured reservoirs[J]. Journal of Natural Gas Science and Engineering, 2016, 30:430-443.

[14] Yang Shangyu. Fracture network fracture mechanics mechanism and productivity prediction of unconventional oil and gas reservoirs [D]. China University of Petroleum (East China), 2015

[15] Olson, J. E., and Dahi-Taleghani, A. 2009. Modeling simultaneous growth of multiple hydraulic fractures and their interaction with natural fractures. SPE 119739, presented at SPE Hydraulic Fracturing Technology Conference, The Woodlands, Texas, USA, 19–21 January.

[16] Olson J E. Fracture aperture, length and pattern geometry development under biaxial loading: a numerical study with applications to natural, cross-jointed systems[J]. Geological Society, London, Special Publications, 2007, 289(1): 123-142.

[17] Kong lie. Numerical simulation of fracture propagation in horizontal wells [D]. Southwest Petroleum University, 2017

[18] Zeng Q, Yao J. Numerical simulation of fracture network generation in naturally fractured reservoirs[J]. Journal of Natural Gas Science & Engineering, 2016, 30:430-443.

[19] Li Yongming, Chen Xiyu, Zhao Jinzhou, et al. Influence of perforation erosion on multiple growing hydraulic fractures in multistage fracturing [J]. Natural Gas Industry, 2017 (7).

[20] Li Yajun, Yao Jun, Huang Chaoqin, et al. Study on permeability characteristics of single fracture porous media [J]. Special oil and gas reservoir, 2011 (04): 98-101 + 144.

[21] Libo. Numerical simulation of embedded discrete fracture model for staged fracturing horizontal well in tight reservoir [D]. Southwest Petroleum University, 2018.

[22] Moinfar A. Developement of an efficient embedded discrete model for 3D compositional reservoir simulation in fractured reservoirs[D]. Texas:the University of Texas at Austin,2013.